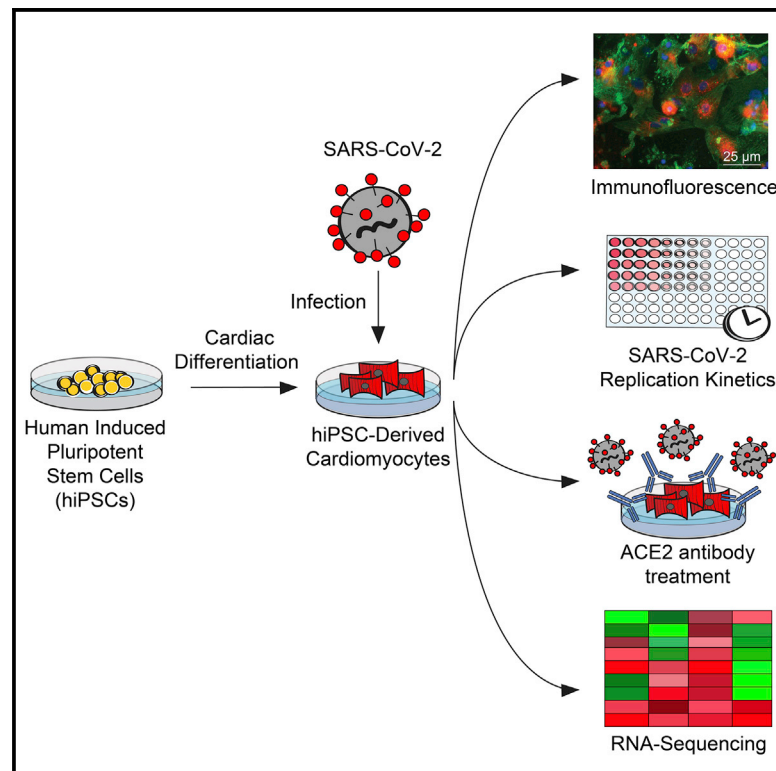**Report**

Human iPSC-Derived Cardiomyocytes Are Susceptible to SARS-CoV-2 Infection

Graphical Abstract

Authors

Arun Sharma, Gustavo Garcia, Jr., Yizhou Wang, Jasmine T. Plummer, Kouki Morizono, Vaithilingaraja Arumugaswami, Clive N. Svendsen

Correspondence

arun.sharma@cshs.org (A.S.), varumugaswami@mednet.ucla.edu (V.A.), clive.svendsen@cshs.org (C.N.S.)

In Brief

Sharma et al. demonstrate that human induced pluripotent stem cell-derived cardiomyocytes (hiPSC-CMs) are susceptible to SARS-CoV-2 infection. This establishes a platform for understanding the mechanisms of cardiac-specific infection by SARS-CoV-2 *in vitro* and could potentially be employed to develop antiviral compounds.

Highlights

- Human iPSC-derived cardiomyocytes are susceptible to SARS-CoV-2 infection

- ACE2 antibody blunts SARS-CoV-2 infection in cardiomyocytes

- Infected human iPSC-derived cardiomyocytes activate viral clearance pathways

CellPress

Cell Reports Medicine

Report

Human iPSC-Derived Cardiomyocytes Are Susceptible to SARS-CoV-2 Infection

Arun Sharma,[1,2,8,*] Gustavo Garcia, Jr.,[3,4] Yizhou Wang,[5] Jasmine T. Plummer,[5] Kouki Morizono,[6,7] Vaithilingaraja Arumugaswami,[3,4,*] and Clive N. Svendsen[1,9,10,*]

[1]Board of Governors Regenerative Medicine Institute, Cedars-Sinai Medical Center, Los Angeles, CA 90048, USA
[2]Smidt Heart Institute, Cedars-Sinai Medical Center, Los Angeles, CA 90048, USA
[3]Department of Molecular and Medical Pharmacology, David Geffen School of Medicine, University of California, Los Angeles, Los Angeles, CA 90095, USA
[4]Eli and Edythe Broad Center of Regenerative Medicine and Stem Cell Research, University of California, Los Angeles, Los Angeles, CA 90095, USA
[5]Genomics Core, Department of Biomedical Sciences, Cedars-Sinai Medical Center, Los Angeles, CA 90048, USA
[6]Division of Hematology and Oncology, Department of Medicine, David Geffen School of Medicine, University of California, Los Angeles, Los Angeles, CA 90095, USA
[7]UCLA AIDS Institute, David Geffen School of Medicine, University of California, Los Angeles, Los Angeles, CA 90095, USA
[8]Twitter: @ArunSharmaPhD
[9]Twitter: @CliveSvendsen
[10]Lead Contact
*Correspondence: arun.sharma@cshs.org (A.S.), varumugaswami@mednet.ucla.edu (V.A.), clive.svendsen@cshs.org (C.N.S.)
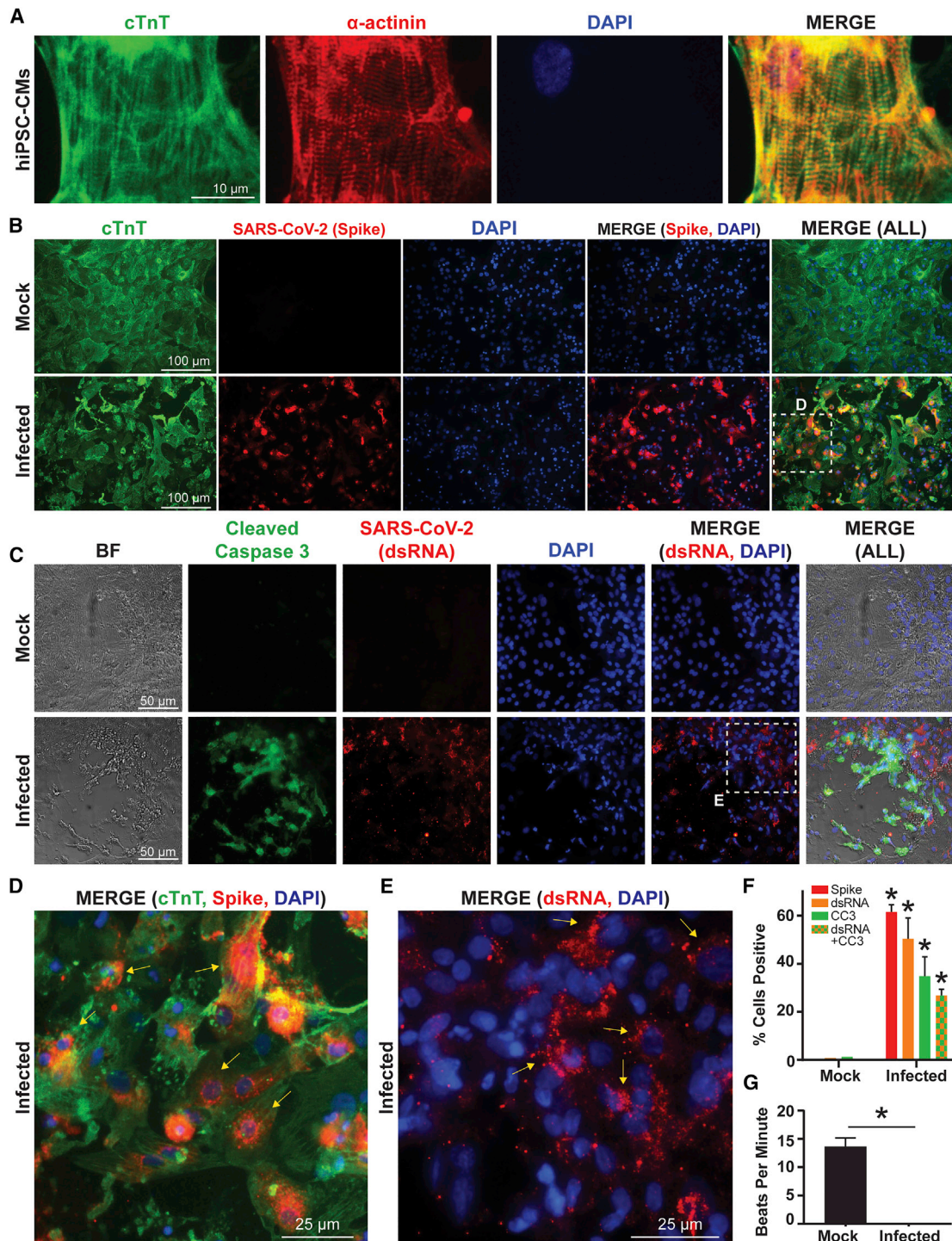 https://doi.org/10.1016/j.xcrm.2020.100052

SUMMARY

Coronavirus disease 2019 (COVID-19) is a pandemic caused by severe acute respiratory syndrome coronavirus 2 (SARS-CoV-2). COVID-19 is defined by respiratory symptoms, but cardiac complications including viral myocarditis are also prevalent. Although ischemic and inflammatory responses caused by COVID-19 can detrimentally affect cardiac function, the direct impact of SARS-CoV-2 infection on human cardiomyocytes is not well understood. Here, we utilize human induced pluripotent stem cell-derived cardiomyocytes (hiPSC-CMs) as a model to examine the mechanisms of cardiomyocyte-specific infection by SARS-CoV-2. Microscopy and RNA sequencing demonstrate that SARS-CoV-2 can enter hiPSC-CMs via ACE2. Viral replication and cytopathic effect induce hiPSC-CM apoptosis and cessation of beating after 72 h of infection. SARS-CoV-2 infection activates innate immune response and antiviral clearance gene pathways, while inhibiting metabolic pathways and suppressing *ACE2* expression. These studies show that SARS-CoV-2 can infect hiPSC-CMs *in vitro*, establishing a model for elucidating infection mechanisms and potentially a cardiac-specific antiviral drug screening platform.

INTRODUCTION

Coronavirus disease 2019 (COVID-19), which is caused by the severe acute respiratory syndrome coronavirus 2 (SARS-CoV-2), has been declared a worldwide pandemic, causing the hospitalization and deaths of hundreds of thousands of people worldwide.[1] SARS-CoV-2, a single-stranded enveloped RNA virus, is known to use the ACE2 receptor to enter host lung tissue, followed by rapid viral replication.[2] Clinical presentation demonstrates predominantly pulmonary symptoms, including cough, shortness of breath, pneumonia, and acute respiratory distress syndrome.[3] However, there is mounting evidence that SARS-CoV-2 infection may cause cardiac complications including elevated cardiac stress biomarkers, arrhythmias, and heart failure.[4] A recent study demonstrated significantly elevated troponin levels among some COVID-19 patients, indicating cardiac injury, and notably, cardiac injury was associated with increased risk of mortality.[5] The etiology of cardiac injury in

COVID-19, however, remains unclear. Cardiac injury may be ischemia mediated, and the profound inflammatory and hemodynamic impacts seen in COVID-19 have been hypothesized to cause atherosclerotic plaque rupture or oxygen supply demand mismatch resulting in ischemia.[3] Alternatively, cardiac tissue expresses the ACE2 receptor, further suggesting the feasibility of direct SARS-CoV-2 internalization in cardiomyocytes (CMs).[6] ACE2 is also upregulated specifically in CMs during dilated and hypertrophic cardiomyopathy.[7] Importantly, the related SARS-CoV virus has been noted to localize within the myocardium,[8] and recent studies[9] have shown 79% sequence conservation in the viral genomes of SARS-CoV and SARS-CoV-2. Structurally, both viruses use the ACE2 receptor to enter cells and bind with similar affinities to ACE2.[10]

Given these similarities to SARS-CoV, it is plausible that SARS-CoV-2 could also use ACE2 to enter adult CMs. Preliminary COVID-19 clinical case reports have raised suspicion for cardiac injury mediated by direct myocardial SARS-CoV-2

Figure 1. SARS-CoV-2 Internalizes and Replicates within hiPSC-CMs *In Vitro*, Eliciting Cytopathic Effect and Contractility Alterations

(A) Human iPSC-CMs exhibit standard sarcomeric markers including cardiac troponin T (cTnT) and α-actinin with DAPI as nuclear counterstain.

(B) Immunofluorescence for cTnT and SARS-CoV-2 "spike" protein demonstrates that hiPSC-CMs can be infected by SARS-CoV-2. SARS-CoV-2 spike protein is not present in mock infected cultures.

(C) HiPSC-CMs after SARS-CoV-2 infection, but not mock infection, exhibit signs of cellular apoptosis, indicated by morphological changes seen in brightfield (BF) and cleaved caspase-3 (CC3) production. A second SARS-CoV-2 antibody marks a viral-specific double-stranded intermediate RNA (dsRNA).

(D) Magnified inset from (B) shows a merged immunofluorescence image for SARS-CoV-2 spike protein, cTnT, and DAPI. Arrows indicate perinuclear accumulation of viral particles and suggest active viral protein translation at perinuclear ribosomes.

(legend continued on next page)

infection and resulting fulminant myocarditis.[11–13] A recent multi-organ autopsy study of COVID-19 patients detected SARS-CoV-2 viral RNA in the heart via PCR.[14] However, the gold standard for confirming SARS-CoV-2 localization in CMs is endomyocardial biopsy (EMB), an invasive procedure, and additional safety precautions also must be taken to conduct EMB in the setting of COVID-19. Thus, there are currently limited clinical data demonstrating localization of SARS-CoV-2 to adult human CMs. In order to gain further insights into the cardiac pathophysiology of COVID-19, it will be critical to determine whether SARS-CoV-2 can directly infect isolated human CMs. Elucidating the pathogenic mechanism of cardiac injury in COVID-19 *in vitro* could ultimately guide therapeutic strategies. Antiviral agents could potentially mitigate cardiac complications if the underlying mechanism of cardiac injury is direct myocardial viral infection.

Primary human CMs are difficult to obtain and maintain for research use. Improved methods to convert human induced pluripotent stem cells (hiPSCs) to multiple somatic lineages have enabled *in vitro* mass production of patient-specific cells, including hiPSC-derived CMs (hiPSC-CMs).[15] The hiPSC-CMs produce relevant proteins found in adult human CMs, can spontaneously contract, can be made in weeks using defined differentiation protocols, and can be genetically customized using genome editing.[16] HiPSC-CMs express *ACE2*, which increases in expression over 90 days of differentiation.[17] The hiPSC-CMs are also responsive to inotropic drugs such as norepinephrine, and beating rates can be controlled via electrical stimulation.[18] Because hiPSC-CMs can be purified and replated for downstream applications, research groups in academia and industry now utilize these cells for cardiovascular disease modeling and high-throughput drug screening assays. HiPSC-CMs can recapitulate cellular phenotypes for cardiovascular diseases including various forms of cardiomyopathy[19,20] and drug-induced cardiotoxicity.[21,22] Notably, hiPSC-CMs have also shown promise as an *in vitro* model for studying the mechanisms of direct CM viral infection in the context of viral myocarditis. A previous study demonstrated that coxsackievirus B3 (CVB3), one of the major causative agents for viral myocarditis, can rapidly infect and proliferate within hiPSC-CMs.[23] CVB3, like SARS-CoV-2, is a positive-sense, single-stranded RNA virus, although unlike SARS-CoV-2, it does not have a viral envelope. The hiPSC-CMs produce the coxsackie and adenovirus receptor protein, which is needed for infection by CVB3. A detrimental virus-induced cytopathic effect was observed in hiPSC-CMs within hours of CVB3 infection, manifesting in cell death and contractility irregularities. Importantly, this study also established hiPSC-CMs as a cardiac-specific antiviral drug screening platform and demonstrated that drugs such as interferon beta and ribavirin can stymie CVB3 proliferation *in vitro*.[23] Interferon beta

was able to transcriptionally activate viral clearance gene networks in CVB3-infected hiPSC-CMs.

Here, the aforementioned foundational viral myocarditis study is extended to assess the effect of SARS-CoV-2 on hiPSC-CMs. We show that hiPSC-CMs are susceptible to SARS-CoV-2 infection, resulting in functional alterations, transcriptional changes, and cytopathic effects. These cellular phenotypes occurred in the absence of systemic inflammatory and hemodynamic impacts, establishing an *in vitro* cardiac platform to study SARS-CoV-2 infection.

RESULTS

hiPSCs Can Differentiate into CMs
An hiPSC control line (02iCTR) was generated by the Cedars-Sinai Medical Center iPSC Core from peripheral blood mononuclear cells and shown to be fully pluripotent.[24] The hiPSCs were differentiated into CMs using an established monolayer differentiation protocol utilizing small molecule modulators of Wnt signaling.[25] Differentiated hiPSC-CMs were metabolically purified by depriving cells of glucose, as previously demonstrated.[25] Purified hiPSC-CMs expressed standard cardiac sarcomeric markers cardiac troponin T (cTnT) and α-actinin (Figure 1A).
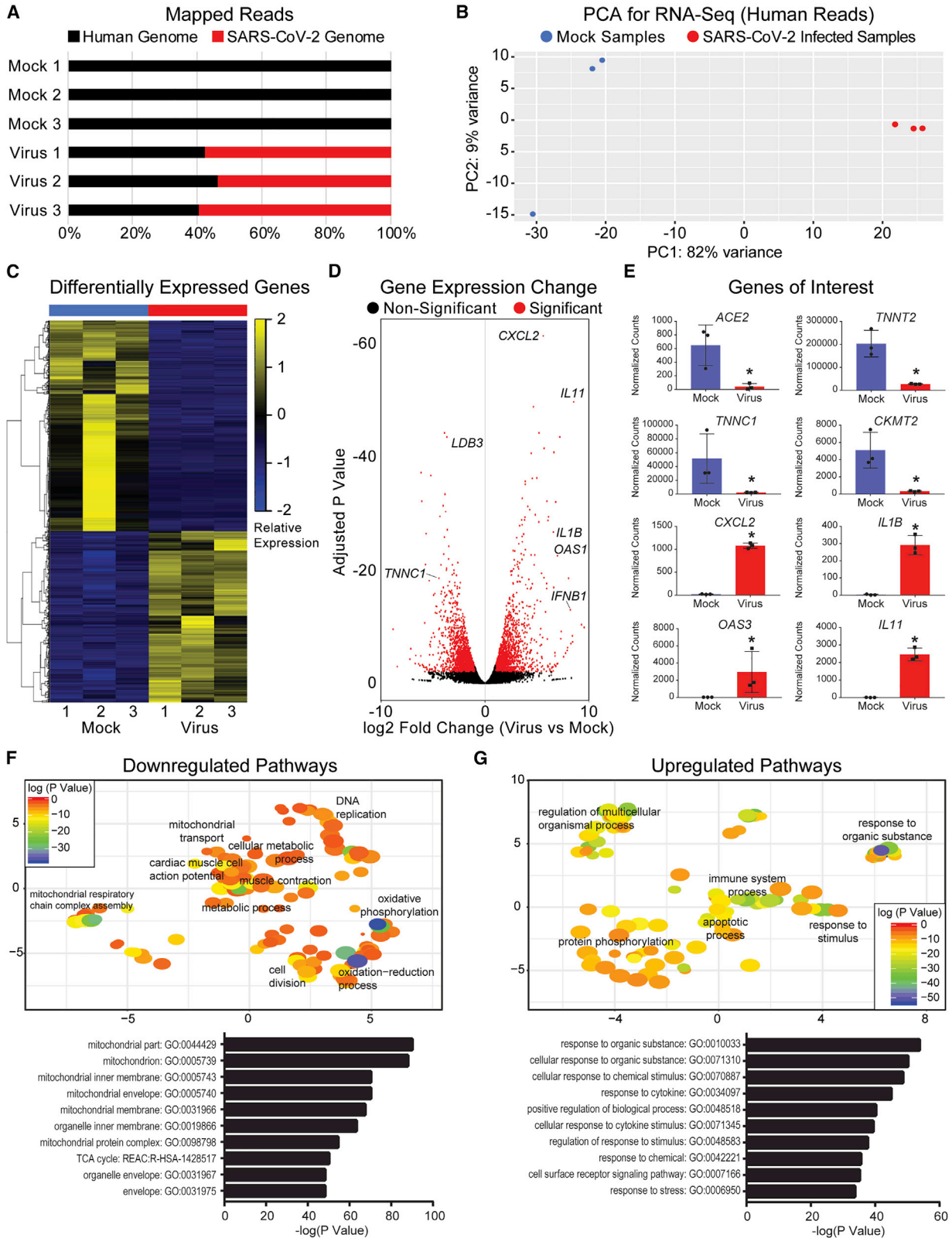
Purified hiPSC-CMs Can Be Directly Infected by SARS-CoV-2
Purified hiPSC-CMs were replated into 96-well plates at 100,000 cells per well and allowed to regain contractility (Video S1) before being subjected to SARS-CoV-2 infection. The SARS-CoV-2 was obtained from the Biodefense and Emerging Infections (BEI) Resources of the National Institute of Allergy and Infectious Diseases (NIAID) and titered on Vero-E6 cells (see STAR Methods). A viral dose response and time course were conducted on hiPSC-CMs, and a multiplicity of infection (MOI) of 0.1 was chosen for all experiments unless otherwise specified (Figure S1). The hiPSC-CMs were infected with SARS-CoV-2 for 72 h in all experiments unless otherwise specified, with a mock treatment without virus serving as a control condition. Plaque formation assays conducted from supernatant harvested after hiPSC-CM infection confirmed active SARS-CoV-2 infection (Figure S1D). Cells from both infected and mock conditions were stained for cardiac marker cTnT and SARS-CoV-2 viral capsid "spike" protein (Figure 1B). The infected hiPSC-CMs stained positively for spike protein, suggesting that SARS-CoV-2 can establish active infection in hiPSC-CMs. As demonstrated previously,[2] pre-treatment of infected hiPSC-CMs with an ACE2 antibody significantly diminished viral protein expression and plaque forming unit production, suggesting that ACE2 is critical for SARS-CoV-2 internalization in hiPSC-CMs (Figure S1).

(E) Magnified inset from (C) shows a merged immunofluorescence image for SARS-CoV-2 dsRNA and DAPI. Arrows indicate dsRNA stain.

(F) Quantification of immunofluorescence indicates percentage of total DAPI-positive cells that are positive for spike protein, viral dsRNA, CC3, and dsRNA+CC3 in hiPSC-CMs infected with SARS-CoV-2, compared to mock infection. n = 5–7 images (technical replicates) quantified for each stain for mock and infected conditions. *p < 0.05.

(G) Quantification of beats per minute in wells containing hiPSC-CMs with mock infection versus wells containing hiPSC-CMs infected with SARS-CoV-2. n = 6 videos (technical replicates) recorded for each condition. See Video S1 for representative video clips. *p < 0.05.

(legend on next page)

Cell Reports Medicine
Report

CellPress
OPEN ACCESS

SARS-CoV-2 Infection of hiPSC-CMs Causes Apoptosis and Cessation of Beating

To determine if SARS-CoV-2 induced a cytopathic effect on hiPSC-CMs, mock and infected hiPSC-CMs were stained for the apoptosis marker cleaved caspase-3, as well as for the double-stranded RNA (dsRNA) intermediate unique to positive sense RNA virus infection (Figure 1C). The dsRNA and spike protein stains represent two independent assays for visualizing SARS-CoV-2 viral uptake and genome replication in hiPSC-CMs. A proportion of infected cells were positive for dsRNA and also stained positive for cleaved caspase-3, indicating that hiPSC-CMs were undergoing virus-induced apoptosis. Pretreatment of infected hiPSC-CMs with an ACE2 antibody significantly reduced cleaved caspase-3 expression and blunted apoptosis (Figure S1). Notably, the SARS-CoV-2 spike protein localized at perinuclear regions in hiPSC-CMs (Figure 1D), consistent with prior results with coronavirus infection in non-CMs[26] and coxsackievirus infection on hiPSC-CMs.[23] The dsRNA intermediates exhibit cytoplasmic localization (Figure 1E). Quantification of stained cells demonstrated the percentage of total cells that were positive for dsRNA and spike protein, as well as for cleaved caspase-3 (Figure 1F). Simple beat rate contractility analysis was also conducted, whereby 30 s videos were taken of wells containing mock and infected hiPSC-CMs (Video S1). Functionally, infected hiPSC-CMs ceased beating after 72 h of SARS-CoV-2 infection, whereas mock wells continued to contract (Figure 1G). Taken together, these results indicate that hiPSC-CMs are susceptible to ACE2-mediated SARS-CoV-2 infection and downstream detrimental cytopathic effects, the SARS-CoV-2 may be able to replicate in distinct perinuclear locations within hiPSC-CMs by co-opting cellular organelles for viral protein translation, and the SARS-CoV-2 infection significantly reduces functional contractility in hiPSC-CMs.

Transcriptional Analysis of SARS-CoV-2-Infected hiPSC-CMs

The hiPSC-CMs infected with 0.1 MOI SARS-CoV-2 for 72 h were also harvested for transcriptomic analysis via RNA sequencing. Upon mapping genomic reads in infected hiPSC-CMs, greater that 50% of all mapped reads were from the SARS-CoV-2 genome, further indicating active SARS-CoV-2 viral genome replication within infected hiPSC-CMs (Figure 2A). Principal component analysis and heatmaps of differentially expressed genes demonstrated clustering of samples by condition (mock or infected) and transcriptomic profile (Figures 2B and 2C). SARS-CoV-2 infection induced significant gene expression changes within hiPSC-CMs (Figure 2D). The most significant expression change by adjusted p value was for *CXCL2*, which encodes an immune cytokine known to be transcriptionally upregulated during SARS-CoV infection.[27] Similarly, immunomodulators such as interleukins were significantly upregulated in infected samples, along with antiviral response pathways genes such as *OAS3*. Expression of CM markers *TNNT2* and *TNNC1* were significantly reduced in infected samples, along with mitochondrial genes related to oxidative phosphorylation, such as *CKMT2*, encoding for creatine kinase. Notably, *ACE2* was significantly downregulated in SARS-CoV-2-infected hiPSC-CMs, consistent with prior reports examining SARS-CoV infection in myocardium.[8] Gene pathway analysis confirmed downregulation of transcriptional pathways related to mitochondrial function, oxidative phosphorylation, and cardiac function, whereas upregulated pathways included responses to organic substance, immune system processes, and apoptosis (Figures 2F and 2G). Taken together, these results indicate that SARS-CoV-2 infection induces significant transcriptional changes within hiPSC-CMs in gene pathways related to cellular metabolism and immune response.

DISCUSSION

Results presented here establish that human iPSC-derived CMs are susceptible to ACE2-mediated direct infection by SARS-CoV-2 and that the virus may induce detrimental cytopathic effects in these cells. At an MOI of 0.1, hiPSC-CMs experienced cytopathic effect after 72 h of infection. The virus presumably enters the cell through the ACE2 receptor, expressed by the hiPSC-CMs in this study. An ACE2 receptor antibody was able to significantly blunt viral protein expression, replication, and cell death. However, in spite of the ACE2 antibody treatment, cells were still susceptible to infection, suggesting potential alternative mechanisms for SARS-CoV-2 internalization. Immunostaining of two SARS-CoV-2 components, the unique dsRNA

Figure 2. SARS-CoV-2 Alters hiPSC-CM Transcriptomic Profiles after Infection

(A) Graph of mapped reads during RNA sequencing. In virus-infected hiPSC-CMs, more than 50% of genomic reads mapped to the SARS-CoV-2 genome, suggesting viral genome presence within infected hiPSC-CMs.

(B) Principal component analysis (PCA) for 3 mock hiPSC-CM samples and 3 SARS-CoV-2-infected hiPSC-CM samples illustrates transcriptional clustering by condition (mock versus infected). Samples represent biological replicates of mock and infected conditions, respectively.

(C) Heatmap of differentially expressed genes shows that samples cluster based on transcriptomic profile and condition (mock versus infected).

(D) Volcano plot of gene expression change in virus-infected versus mock samples. Significantly changed gene are defined with adjusted p < 0.01 and absolute value fold change >2. Genes of interest noted include cardiac markers *LDB3* and *TNNC1*, cytokines *CXCL2*, *IL11*, *IL1B*, and *IFNB1*, and antiviral response gene *OAS1*.

(E) Expression of genes of interest in mock versus infected conditions. *TNNT2* and *TNNC1* represent cardiac markers, whereas *CKMT2* represents mitochondrial enzymes. *CXCL2*, *IL1B*, *IL11*, and *OAS3* represent innate immune response and viral clearance genes. *p < 0.05.

(F) Top: downregulated transcriptional pathways based on Gene Ontology (GO) analysis, visualized using REViGO. Significantly downregulated pathways include mitochondrial transport, oxidative phosphorylation, oxidation-reduction processes, and muscle contraction. Bottom: top 10 most significant GO terms associated with downregulated pathways are related to mitochondrial function.

(G) Top: upregulated transcriptional pathways based on GO analysis, visualized using REViGO. Significantly upregulated pathways include response to organic substance, immune system process, and apoptotic process. Bottom: top 10 most significant GO terms associated with upregulated pathways are related to response to organic stimulus.

intermediate and the "spike" capsid protein responsible for viral entry and virion particle assembly, demonstrates that this novel coronavirus can enter hiPSC-CMs to unleash its RNA cargo and hijack host hiPSC-CM translational machinery to produce new viral components. Notably, the "spike" protein stain localized to perinuclear regions, likely near the endoplasmic reticulum. Not only has this perinuclear viral component accumulation been reported in other *in vitro* coronavirus infection studies,[26] but it parallels what was seen in hiPSC-CMs infected with CVB3.[23] Presumably, this increased viral load within hiPSC-CMs activated downstream apoptotic events. This was indicated by alterations in cellular morphologies, increased production of cleaved caspase-3, and activation of cell death gene networks.

In parallel with these stains showing viral accumulation, there was a functional alteration in hiPSC-CM contractility where the cells ceased beating. The cause of this dramatic functional change in hiPSC-CM beating must be further investigated, but perhaps cytopathic effect and associated hiPSC-CM apoptosis significantly disrupted cell-cell gap junctions and therefore impaired proper excitation-contraction coupling within and between CMs. Indeed, significant alterations in calcium handling and contractility were similarly observed in CVB3-infected hiPSC-CMs.[23] Additionally, SARS-CoV-2 induced widespread transcriptional changes in infected hiPSC-CMs. Paralleling findings from SARS-CoV infection studies, SARS-CoV-2 infection on CMs downregulated the expression of *ACE2*[8] and upregulated expression of *CXCL2*,[27] along with other immunomodulatory cytokines. Reduction in cardiac-specific contractile genes such as *TNNT2* likely reflects the impairment in contractility of infected hiPSC-CMs, as well as overall CM death. Infected hiPSC-CMs also experienced profound downregulation in gene networks associated with oxidative phosphorylation and mitochondrial function, consistent with the dramatic metabolic impacts that viral infections elicit.[28]

We predict that future studies will be able to use hiPSC-CMs as a cardiac-specific antiviral drug screening platform, in similar fashion to previous studies with CVB3 on hiPSC-CMs.[23] A variety of antiviral approaches ranging from repurposed small molecules, such as nucleoside analogs or viral polymerase inhibitors, to novel antibodies and antisense oligonucleotides have been proposed for COVID-19 and are currently being tested *in vitro* and in clinical trials.[29] HiPSC-CMs could serve as a cardiac-specific auxiliary cell type for *in vitro* pre-clinical efficacy studies for any drug aiming to stymie SARS-CoV-2 proliferation. In parallel, drug-induced arrhythmias and QT-interval prolongation can also be examined for antiviral compounds in pre-clinical development, given that some existing COVID-19 drug treatments exhibit these off-target cardiotoxicities.[30] Due to the enormity of the current COVID-19 pandemic, and the increasing evidence for associated cardiac symptoms, innovative approaches using technologies such as the hiPSC-CMs presented here will be critical to further understand and counteract SARS-CoV-2 infection.

Limitations of Study

The cellular immaturity of hiPSC-derivative cell types must be considered in this model. It is known that hiPSC-CMs are electrophysiologically, structurally, and genetically immature in comparison to their adult counterparts,[31] although biomechanical efforts to mature these cells toward an adult phenotype have recently gained traction.[32] However, even in these immature cells, the current study showed overt virus-induced cardiotoxicity and physiological effects at SARS-CoV-2 MOIs ranging from 0.001 to 0.1. Since expression of *ACE2* increases as hiPSC-CMs mature in *in vitro* culture,[17] one could hypothesize that after maturation, older hiPSC-CMs would be even more susceptible to SARS-CoV-2 infection. Significant additional data are needed to test these possibilities.

The results presented here are in an isolated *in vitro* system, devoid of any immune system cellular components that are thought to be critical to the many aspects of the COVID-19 viral response *in vivo*.[33] The resulting myocarditis, by definition, is an inflammation of the myocardium caused by immune cell infiltration, which may or may not be the result of direct CM viral infection. However, as shown here, hiPSC-derived CMs are clearly susceptible to SARS-CoV-2 infection even in the absence of a cellular immune response. Still, current clinical data have not definitively established direct infection of the heart playing a role in the clinical syndrome. Although studies presenting EMBs from COVID-19 patients are rare at this point, biopsied heart tissue has shown the SARS-CoV-2 virus localizing in the heart of a COVID-19 patient, albeit not specifically in the CMs.[13] A recent multi-organ autopsy study also showed SARS-CoV-2 viral RNA in the heart.[14] Additional clinical data are needed, but this raises the question of whether the SARS-CoV-2 enters the heart via a viremic phase or through macrophages clearing the virus from the lungs. It remains to be seen whether direct CM infection may contribute to the variety of *in vivo* cardiac clinical sequelae presented by patients with COVID-19, such as arrhythmias, elevated cardiac troponin biomarkers, or heart failure. Nonetheless, we establish that hiPSC-CMs *in vitro* are susceptible to SARS-CoV-2 infection.

STAR★METHODS

Detailed methods are provided in the online version of this paper and include the following:

- KEY RESOURCES TABLE
- RESOURCE AVAILABILITY
  - Lead Contact
  - Materials Availability
  - Data and Code Availability
- EXPERIMENTAL MODEL AND SUBJECT DETAILS
  - HiPSC derivation
  - SARS-CoV-2 isolate
  - Vero-E6 cells
- METHOD DETAILS
  - HiPSC-CM differentiation
  - SARS-CoV-2 expansion in Vero-E6 cells
  - SARS-CoV-2 infection of hiPSC-CMs
  - Imaging and immunofluorescence
  - SARS-CoV-2 growth kinetics time course
  - Viral plaque formation assay
  - Blocking ACE2 with antibody

Cell Reports Medicine
Report

CellPress
OPEN ACCESS

- ○ RNA-Sequencing
- ○ Bioinformatics and data analysis
- ○ Beat rate analysis
- ● QUANTIFICATION AND STATISTICAL ANALYSIS

REFERENCES

1. Ramaiah, A., and Arumugaswami, V. (2020). Insights into Cross-species Evolution of Novel Human Coronavirus 2019-nCoV and Defining Immune Determinants for Vaccine Development. bioRxiv. https://doi.org/10.1101/2020.01.29.925867.

2. Hoffmann, M., Kleine-Weber, H., Schroeder, S., Kruger, N., Herrler, T., and Erichsen, S., Schiergens, T.S., Herrler, G., Wu, N.-H., Nitsche, A., Müller, M.A., et al. SARS-CoV-2 Cell Entry Depends on ACE2 and TMPRSS2 and Is Blocked by a Clinically Proven Protease Inhibitor. Cell 181, 271–280.

3. Madjid, M., Safavi-Naeini, P., Solomon, S.D., and Vardeny, O. (2020). Potential Effects of Coronaviruses on the Cardiovascular System: A Review. JAMA Cardiol. Published online: March 27, 2020. https://doi.org/10.1001/jamacardio.2020.1286.

4. Fried, J.A., Ramasubbu, K., Bhatt, R., Topkara, V.K., Clerkin, K.J., Horn, E., Rabbani, L., Brodie, D., Jain, S.S., Kirtane, A.J., et al. (2020). The Variety of Cardiovascular Presentations of COVID-19. Circulation 141, 1930–1936.

5. Shi, S., Qin, M., Shen, B., Cai, Y., Liu, T., Yang, F., Gong, W., Liu, X., Liang, J., Zhao, Q., et al. (2020). Association of Cardiac Injury With Mortality in Hospitalized Patients With COVID-19 in Wuhan, China. JAMA Cardiol. Published online: March 25, 2020. https://doi.org/10.1001/jamacardio.2020.0950.

6. Chen, L., Li, X., Chen, M., Feng, Y., and Xiong, C. (2020). The ACE2 expression in human heart indicates new potential mechanism of heart injury among patients infected with SARS-CoV-2. Cardiovasc. Res. 116, 1097–1100.

7. Tucker, N.R., Chaffin, M., Bedi, K.C., Papangeli, I., Akkad, A.-D., Arduini, A., Hayat, S., Eraslan, G., Muus, C., Bhattacharyya, R., et al. (2020). Myocyte Specific Upregulation of ACE2 in Cardiovascular Disease: Implications for SARS-CoV-2 mediated myocarditis. medRxiv, doi: 2020.04.09.20059204.

8. Oudit, G.Y., Kassiri, Z., Jiang, C., Liu, P.P., Poutanen, S.M., Penninger, J.M., and Butany, J. (2009). SARS-coronavirus modulation of myocardial ACE2 expression and inflammation in patients with SARS. Eur. J. Clin. Invest. 39, 618–625.

9. Lu, R., Zhao, X., Li, J., Niu, P., Yang, B., Wu, H., Wang, W., Song, H., Huang, B., Zhu, N., et al. (2020). Genomic characterisation and epidemiology of 2019 novel coronavirus: implications for virus origins and receptor binding. Lancet 395, 565–574.

10. Walls, A.C., Park, Y.J., Tortorici, M.A., Wall, A., McGuire, A.T., and Veesler, D. (2020). Structure, Function, and Antigenicity of the SARS-CoV-2 Spike Glycoprotein. Cell 181, 281–292.

11. Hu, H., Ma, F., Wei, X., and Fang, Y. (2020). Coronavirus fulminant myocarditis saved with glucocorticoid and human immunoglobulin. Eur. Heart J., ehaa190.

12. Zeng, J.H., Liu, Y.X., Yuan, J., Wang, F.X., Wu, W.B., Li, J.X., Wang, L.F., Gao, H., Wang, Y., Dong, C.F., et al. (2020). First case of COVID-19 complicated with fulminant myocarditis: a case report and insights. Infection, Published online April 10, 2020. https://doi.org/10.1007/s15010-020-01424-5.

13. Tavazzi, G., Pellegrini, C., Maurelli, M., Belliato, M., Sciutti, F., Bottazzi, A., Sepe, P.A., Resasco, T., Camporotondo, R., Bruno, R., et al. (2020). Myocardial localization of coronavirus in COVID-19 cardiogenic shock. Eur. J. Heart Fail. 22, 911–915.

14. Puelles, V.G., Lütgehetmann, M., Lindenmeyer, M.T., Sperhake, J.P., Wong, M.N., Allweiss, L., Chilla, S., Heinemann, A., Wanner, N., Liu, S., et al. (2020). Multiorgan and Renal Tropism of SARS-CoV-2. N. Engl. J. Med. Published online May 13, 2020. https://doi.org/10.1056/NEJMc2011400.

15. Sharma, A., Sances, S., Workman, M.J., and Svendsen, C.N. (2020). Multilineage Human iPSC-Derived Platforms for Disease Modeling and Drug Discovery. Cell Stem Cell 26, 309–329.

16. Sharma, A., Toepfer, C.N., Ward, T., Wasson, L., Agarwal, R., Conner, D.A., et al. (2018). CRISPR/Cas9-Mediated Fluorescent Tagging of Endogenous Proteins in Human Pluripotent Stem Cells. Curr. Protoc. Hum. Genet. 96, 21.11.1–21.11.20.

17. Churko, J.M., Garg, P., Treutlein, B., Venkatasubramanian, M., Wu, H., Lee, J., Wessells, Q.N., Chen, S.Y., Chen, W.Y., Chetal, K., et al. (2018). Defining human cardiac transcription factor hierarchies using integrated single-cell heterogeneity analysis. Nat. Commun. 9, 4906.

18. Toepfer, C.N., Sharma, A., Cicconet, M., Garfinkel, A.C., Mücke, M., Neyazi, M., Willcox, J.A.L., Agarwal, R., Schmid, M., Rao, J., et al. (2019). SarcTrack. Circ. Res. 124, 1172–1183.

19. Lan, F., Lee, A.S., Liang, P., Sanchez-Freire, V., Nguyen, P.K., Wang, L., Han, L., Yen, M., Wang, Y., Sun, N., et al. (2013). Abnormal calcium handling properties underlie familial hypertrophic cardiomyopathy pathology in patient-specific induced pluripotent stem cells. Cell Stem Cell 12, 101–113.

20. Sun, N., Yazawa, M., Liu, J., Han, L., Sanchez-Freire, V., Abilez, O.J., Navarrete, E.G., Hu, S., Wang, L., Lee, A., et al. (2012). Patient-specific induced pluripotent stem cells as a model for familial dilated cardiomyopathy. Sci. Transl. Med. 4, 130ra47.

21. Sharma, A., Burridge, P.W., McKeithan, W.L., Serrano, R., Shukla, P., Sayed, N., Churko, J.M., Kitani, T., Wu, H., Holmström, A., et al. (2017). High-throughput screening of tyrosine kinase inhibitor cardiotoxicity with human induced pluripotent stem cells. Sci. Transl. Med. 9, eaaf2584.

22. Burridge, P.W., Li, Y.F., Matsa, E., Wu, H., Ong, S.G., Sharma, A., Holmström, A., Chang, A.C., Coronado, M.J., Ebert, A.D., et al. (2016). Human induced pluripotent stem cell-derived cardiomyocytes recapitulate the predilection of breast cancer patients to doxorubicin-induced cardiotoxicity. Nat. Med. *22*, 547–556.

23. Sharma, A., Marceau, C., Hamaguchi, R., Burridge, P.W., Rajarajan, K., Churko, J.M., Wu, H., Sallam, K.I., Matsa, E., Sturzu, A.C., et al. (2014). Human induced pluripotent stem cell-derived cardiomyocytes as an in vitro model for coxsackievirus B3-induced myocarditis and antiviral drug screening platform. Circ. Res. *115*, 556–566.

24. Laperle, A.H., Sances, S., Yucer, N., Dardov, V.J., Garcia, V.J., Ho, R., Fulton, A.N., Jones, M.R., Roxas, K.M., Avalos, P., et al. (2020). iPSC modeling of young-onset Parkinson's disease reveals a molecular signature of disease and novel therapeutic candidates. Nat. Med. *26*, 289–299.

25. Sharma, A., Li, G., Rajarajan, K., Hamaguchi, R., Burridge, P.W., and Wu, S.M. (2015). Derivation of highly purified cardiomyocytes from human induced pluripotent stem cells using small molecule-modulated differentiation and subsequent glucose starvation. J. Vis. Exp. Published online: March 18, 2015. https://doi.org/10.3791/52628.

26. Hagemeijer, M.C., Vonk, A.M., Monastyrska, I., Rottier, P.J., and de Haan, C.A. (2012). Visualizing coronavirus RNA synthesis in time by using click chemistry. J. Virol. *86*, 5808–5816.

27. Versteeg, G.A., van de Nes, P.S., Bredenbeek, P.J., and Spaan, W.J. (2007). The coronavirus spike protein induces endoplasmic reticulum stress and upregulation of intracellular chemokine mRNA concentrations. J. Virol. *81*, 10981–10990.

28. Thaker, S.K., Ch'ng, J., and Christofk, H.R. (2019). Viral hijacking of cellular metabolism. BMC Biol. *17*, 59.

29. Harrison, C. (2020). Coronavirus puts drug repurposing on the fast track. Nat. Biotechnol. *38*, 379–381.

30. Roden, D.M., Harrington, R.A., Poppas, A., and Russo, A.M. (2020). Considerations for Drug Interactions on QTc in Exploratory COVID-19 (Coronavirus Disease 2019) Treatment. Circulation *141*, e906–e907.

31. Bedada, F.B., Wheelwright, M., and Metzger, J.M. (2016). Maturation status of sarcomere structure and function in human iPSC-derived cardiac myocytes. Biochim. Biophys. Acta *1863* (*7 Pt B*), 1829–1838.

32. Ronaldson-Bouchard, K., Ma, S.P., Yeager, K., Chen, T., Song, L., Sirabella, D., Morikawa, K., Teles, D., Yazawa, M., and Vunjak-Novakovic, G. (2018). Advanced maturation of human cardiac tissue grown from pluripotent stem cells. Nature *556*, 239–243.

33. Shi, Y., Wang, Y., Shao, C., Huang, J., Gan, J., Huang, X., Bucci, E., Piacentini, M., Ippolito, G., and Melino, G. (2020). COVID-19 infection: the perspectives on immune responses. Cell Death Differ. *27*, 1451–1454.

34. LaBarre, D.D., and Lowy, R.J. (2001). Improvements in methods for calculating virus titer estimates from TCID50 and plaque assays. J. Virol. Methods *96*, 107–126.

35. Dobin, A., Davis, C.A., Schlesinger, F., Drenkow, J., Zaleski, C., Jha, S., Batut, P., Chaisson, M., and Gingeras, T.R. (2013). STAR: ultrafast universal RNA-seq aligner. Bioinformatics *29*, 15–21.

36. Li, B., and Dewey, C.N. (2011). RSEM: accurate transcript quantification from RNA-Seq data with or without a reference genome. BMC Bioinformatics *12*, 323.

37. Supek, F., Bošnjak, M., Škunca, N., and Šmuc, T. (2011). REVIGO summarizes and visualizes long lists of gene ontology terms. PLoS ONE *6*, e21800.

STAR★METHODS

KEY RESOURCES TABLE

REAGENT or RESOURCE	SOURCE	IDENTIFIER
Antibodies		
α-actinin	Sigma-Aldrich	Cat# A7811, RRID: AB_476766
cardiac troponin T	Abcam	Cat# ab45932, RRID: AB_956386
SARS-CoV-2 spike (S) protein	BEI Resources	NR-616 Monoclonal Anti-SARS-CoV S Protein (Similar to 240C) SARS coronavirus
SARS-CoV-2 double stranded RNA	Absolute Antibody Inc	J2 clone
cleaved caspase-3	Cell Signaling Technology	Cat# 9661, RRID: AB_2341188
donkey anti-rabbit 488	Thermo Fisher Scientific	at# R37118, RRID: AB_2556546
goat anti-mouse 555	Thermo Fisher Scientific	Cat# A32727, RRID: AB_2633276
donkey anti-mouse 594	Thermo Fisher Scientific	Cat# R37115, RRID: AB_2556543
ACE2	R&D Systems	Cat# AF933, RRID: AB_355722
TIM4	R&D Systems	Cat# AF2929, RRID: AB_2240431
Bacterial and Virus Strains		
SARS-CoV-2	Biodefense and Emerging Infections (BEI) Resources of the National Institute of Allergy and Infectious Diseases (NIAID)	isolate USA-WA1/2020
Chemicals, Peptides, and Recombinant Proteins		
mTeSR1	STEMCELL Technologies	mTeSR1
CHIR99021	Cayman Chemical	252917-06-9
Wnt-C59	Cayman Chemical	1243243-89-1
RPMI 1640	Thermo Fisher Scientific	11875093
RPMI 1640 no glucose	Thermo Fisher Scientific	11879020
B27 supplement minus insulin	Thermo Fisher Scientific	A1895601
B27 supplement with insulin	Thermo Fisher Scientific	17504044
DMEM/F-12, HEPES	Thermo Fisher Scientific	11330057
Matrigel	Corning	cat. # 354230
Phosphate Buffered Saline	GIBCO	cat. # 10010023
Fetal Bovine Serum	Millipore Sigma	F2442
HEPES Buffer Solution	Millipore Sigma	83264
Penicillin/Streptomycin	Millipore Sigma	P4333
4% paraformaldehyde solution	Fisher Scientific	AAJ19943K2
Bovine Serum Albumin	Millipore Sigma	A1933
Normal Donkey Serum	Abcam	Ab7475
Normal Goat Serum	Abcam	Ab7481
Triton X-100	Millipore Sigma	X100
DAPI	Millipore Sigma	MBD0015
Trizol	Thermo Fisher Scientific	15596026
L-Glutamine	Thermo Fisher Scientific	25030081
Critical Commercial Assays		
RNeasy mini kit	QIAGEN	cat. # 74104
SMART-Seq V4 Ultra Low RNA Input Kit	Takara Bio USA	R400752
Nextera XT Library Preparation kit	Illumina	FC-131-1024
Deposited Data		
Raw genomic data	This paper	GSE150392

(Continued on next page)

Continued

REAGENT or RESOURCE	SOURCE	IDENTIFIER
Experimental Models: Cell Lines		
02iCTR hiPSC line	Cedars-Sinai Medical Center (Laperle et al., 2020)	02iCTR
Vero-E6	ATCC	CRL-1586
Software and Algorithms		
ImageJ (Fiji)	NIH	https://imagej.nih.gov/ij/docs/guide/146-2.html
GraphPad Prism (8.0)	GraphPad	https://www.graphpad.com/scientific-software/prism/
Microsoft Excel	Microsoft	https://www.microsoft.com/en-us/microsoft-365/p/excel/cfq7ttc0k7dx?activetab=pivot%3aoverviewtab
Adobe Photoshop(CC)	Adobe	https://www.adobe.com/products/photoshop.html
Adobe Illustrator (CC)	Adobe	https://www.adobe.com/products/illustrator.html
STAR (version 2.5.0)	Github	https://github.com/alexdobin/STAR/releases
SARS-CoV-2 viral genome MT246667.1	NIH GenBank	https://www.ncbi.nlm.nih.gov/nuccore/MT246667.1
R version 3.6.3	R project	https://www.r-project.org/
REViGO	Rudjer Boskovic Institute, Croatia	http://revigo.irb.hr/

RESOURCE AVAILABILITY

Lead Contact
Further information and requests for resources and reagents should be directed to and will be fulfilled by the Lead Contact, Clive Svendsen (Clive.Svendsen@cshs.org).

Materials Availability
This study did not generate new unique reagents.

Data and Code Availability
The gene expression data from this study are found at Gene Expression Omnibus with accession number GSE150392.

EXPERIMENTAL MODEL AND SUBJECT DETAILS

HiPSC derivation
The appropriate institutional review board (IRB) and stem cell research oversight committee (SCRO) were consulted at UCLA and Cedars-Sinai Medical Center. The 02iCTR hiPSC line (male, clinically normal, no known associated disease) was derived from human peripheral blood mononuclear cells and has been published previously.[24] This cell line was obtained from the Cedars-Sinai Medical Center iPSC core facility and was derived using non-integrating episomal reprogramming under their IRB-SCRO protocol "Pro00032834: iPSC Core Repository and Stem Cell Program." These hiPSCs were grown on Matrigel and maintained in mTeSR1 (STEMCELL Technologies). Cells were maintained at approximately passage 30-40 during differentiation, with daily replacement of mTeSR1 and manual passaging after reaching 80% confluency (approximately every 4 days).

SARS-CoV-2 isolate
SARS-CoV-2, isolate USA-WA1/2020, was obtained from the Biodefense and Emerging Infections (BEI) Resources of the National Institute of Allergy and Infectious Diseases (NIAID). Importantly, all studies involving SARS-CoV-2 infection of hiPSC-CMs were conducted within a Biosafety Level 3 facility at UCLA.

Cell Reports Medicine
Report

Vero-E6 cells
Vero-E6 cell line was obtained from the American Type Culture Collection (ATCC) cell line catalog, under catalog number VERO C1008 [Vero 76, clone E6, Vero E6] (ATCC CRL1586). These are immortalized adherent kidney epithelial cells from *Cercopithecus aethiops*, the African green monkey.

METHOD DETAILS

HiPSC-CM differentiation
The hiPSC differentiation work in the Svendsen Lab is carried out under "Pro00021505: Svendsen Stem Cell Program," authorized by the Cedars-Sinai Medical Center IRB. Initially, hiPSCs were grown on Matrigel and maintained in mTeSR1 (STEMCELL Technologies). The hiPSC-CMs were generated from hiPSCs using a small-molecule mediated differentiation approach that modulates Wnt signaling.[25] Briefly, this approach uses the CHIR99021 GSK3β inhibitor from days 0-2 to initiate mesoderm specification, followed by Wnt-C59 Wnt inhibitor at days 3-5 to initiate cardiac specification. From days 0-7 of differentiation, cells are maintained in RPMI 1640 + B27 supplement without insulin. Cells began beating at approximately day 7 post-differentiation, at which point medium was changed to RPMI 1640 + B27 supplement with insulin. Cardiomyocytes were metabolically selected from other differentiated cells by conducting glucose deprivation in RPMI 1640 without glucose + B27 supplement with insulin as previously described.[25] After selection, hiPSC-CMs were replated as a monolayer into 96-well plate format at 100,000 cells per well in hiPSC-CM culture medium, RPMI 1640 + B27 supplement with insulin.

SARS-CoV-2 expansion in Vero-E6 cells
SARS-CoV-2 was passaged once in Vero-E6 cells (ATCC) and viral stocks were aliquoted and stored at −80°C. Virus titer was measured in Vero-E6 cells by $TCID_{50}$ assay. Vero-E6 cells were cultured in DMEM growth media containing 10% fetal bovine serum, 2 mM L-glutamine, penicillin (100 units/ml), streptomycin (100 units/ml), and 10 mM HEPES. Cells were incubated at 37°C with 5% CO_2.

SARS-CoV-2 infection of hiPSC-CMs
For hiPSC-CM infection, viral inoculum (MOI of 0.1, or 1 plaque forming unit per 10 cells) was prepared using serum-free media, unless otherwise specified. Culture media from each well containing hiPSC-CMs was removed and replaced with 250 μL of prepared inoculum. For mock infection, serum-free media (250 μL/well) alone was added. The inoculated plates were incubated for 1 hour at 37°C with 5% CO_2. The inoculum was spread by gently tilting the plate sideways every 15 minutes. At the end of incubation, the inoculum was replaced with fresh hiPSC-CM culture medium. Cells remained at 37°C with 5% CO_2 for 72 hours before analysis.

Imaging and immunofluorescence
After 72 hours of SARS-CoV-2 infection (or mock), live cell images and videos were obtained by bright field microscope (Leica DMIL LED). For immunofluorescence, separate wells of hiPSC-CMs were fixed with 4% paraformaldehyde in phosphate-buffered saline (PBS) for 20 minutes. The fixed samples were then permeabilized and blocked for 1 hour in a "blocking solution" containing PBS with 2% bovine serum albumin, 5% donkey serum, 5% goat serum, and 0.3% Triton X-100. Primary antibodies were diluted in the blocking solution and added to samples overnight at 4°C. The following antibodies and dilutions were used: α-actinin (1:100, Sigma-Aldrich Cat# A7811, RRID: AB_476766); cardiac troponin T (cTnT, 1:100, Abcam Cat# ab45932, RRID: AB_956386); SARS-CoV-2 spike (S) protein (1:100, BEI Resources NR-616 Monoclonal Anti-SARS-CoV S Protein (Similar to 240C) SARS coronavirus); SARS-CoV-2 double stranded RNA (1:100, J2 clone; Absolute Antibody Inc.); cleaved caspase-3 (1:200, Cell Signaling Technology Cat# 9661, RRID: AB_2341188). Samples were then rinsed 5 times for 2 minutes each with PBS containing 0.3% Triton X-100, followed by incubation with fluorescent-conjugated secondary antibodies diluted 1:1000 in blocking buffer for 2 hours at room temperature. Antibodies were donkey anti-rabbit 488 (Thermo Fisher Scientific Cat# R37118, RRID: AB_2556546), goat anti-mouse 555 (Thermo Fisher Scientific Cat# A32727, RRID: AB_2633276), and donkey anti-mouse 594 (Thermo Fisher Scientific Cat# R37115, RRID: AB_2556543). Samples were then rinsed 5 times for 2 minutes each with PBS containing 0.3% Triton X-100, followed by DAPI diluted in PBS at 1:5000 for 10 minutes. Immunofluorescence images were quantified using ImageJ software. DAPI was used to count total cell numbers in order to obtain a percentage of cells positive for dsRNA, spike protein, or cleaved caspase-3.

SARS-CoV-2 growth kinetics time course
The hiPSC-CMs were infected with SARS-CoV-2 at varying MOIs of 0.1, 0.01 and 0.001 in 96-well plate (Figure S1C). Mock infected cells received only the media used for preparing the SARS-CoV-2 inoculum. After 1-hour incubation at 37°C with 5% CO_2, the inocula were replaced with fresh media followed by PBS (phosphate buffered saline) wash. At each time point (days 1, 2 and 3), cell culture supernatant samples from mock and SARS-CoV-2 infected wells were collected and stored at −80°C. Viral production by infected hiPSC-CMs at each time point was measured by quantifying $TCID_{50}$ (Median Tissue Culture Infectious Dose). In brief, Vero-E6 cells were plated in 96-well plate at a density of 5 x10^3 cells/well. The next day, culture supernatants collected from hiPSC-CMs at various time points were subjected to 10-fold serial dilutions (10^{-1} to 10^{-6}) and inoculated onto Vero-E6 cells. The cells were incubated at 37°C with 5% CO_2. After 72 hours, each inoculated well was examined for presence or absence of viral cytopathic effect and percent

infected dilutions immediately above and immediately below 50% were determined. $TCID_{50}$ was calculated as described previously.[34] $TCID_{50}$ values of each viral MOIs at different time points were subjected to statistical analysis and plotted in a line graph.

Viral plaque formation assay

To quantify virus titer after 72 hour SARS-CoV-2 infection dose response on hiPSC-CMs (Figure S1), culture supernatants from each MOI condition were subjected to 10-fold serial dilutions and added to Vero-E6 cells in a 96-well plate. At 48 hours post infection on Vero-E6, the cells were fixed in methanol and subjected to immunostaining using dsRNA antibody. Immunostained viral plaques were counted in the highest viral dilution-containing wells. Plaque forming unit per milliliter (PFU/mL) of culture supernatant was calculated for each condition.

Blocking ACE2 with antibody

The hiPSC-CMs were pre-treated with anti-ACE2 antibody (R&D Systems Cat# AF933, RRID: AB_355722; 20 μg/well in 100 μL media) for 1 hour. Untreated hiPSC-CMs and non-specific antibody (anti-TIM4 antibody, R&D Systems Cat# AF2929, RRID: AB_2240431; 20 μg/well in 100 μL media) treated cells were included as controls. After 1 hour of antibody pre-treatment at 37°C, SARS-CoV-2 viral inoculum (MOI of 0.01) was added to each well. Subsequently at 1-hour post-infection (hpi), virus inoculum was replaced with fresh media. 72 hours later, the cells were fixed with 4% paraformaldehyde for immunofluorescence analysis.

RNA-Sequencing

After 72-hour viral treatment, cells designated for transcriptomic analysis were harvested in Trizol and total RNA extracted using a QIAGEN RNEasy Mini Kit. Total RNA was then used for library preparation and sequencing. The SMART-Seq V4 Ultra Low RNA Input Kit for Sequencing (Takara Bio USA, Inc., Mountain View, CA) was used for reverse transcription and generation of double stranded cDNA for library preparation using the Nextera XT Library Preparation kit (Illumina, San Diego, CA). Total RNA quality was analyzed via the 2100 Bioanalyzer (Agilent Technologies, Santa Clara, CA) and RNA quantified using QubitTM (ThermoFisher Scientific, Waltham, MA) fluorometric quantitation. An input of 10 ng total RNA was used for oligo(dT)-primed reverse transcription, cDNA amplification, and cDNA cleanup. The cDNA was analyzed on the 4200 TapeStation (Agilent Technologies). Quantification of cDNA was performed using Qubit. cDNA normalized to 30 pg/mL was fragmented and sequencing primers added simultaneously. A limiting-cycle PCR added Index 1 (i7) adapters, Index 2 (i5) adapters, and sequences required for cluster formation on the sequencing flow cell. Indexed libraries were cleaned up, library size verification performed on the 4200 TapeStation, and library quantified via Qubit. Libraries were sequenced on a NextSeq 500 using with a 1x75 bp read length and coverage of ∼60M reads/cell.

Bioinformatics and data analysis

Raw reads obtained from RNA-Seq were aligned to the transcriptome using STAR (version 2.5.0)[35] / RSEM (version 1.2.25)[36] with default parameters, using a custom human GRCh38 transcriptome reference downloaded from https://www.gencodegenes.org, containing all protein coding and long non-coding RNA genes based on human GENCODE version 33 annotation. For SARS-CoV-2 viral genome alignment, GenBank: MT246667.1 reference sequence was used. Expression counts for each gene in all samples were normalized by a modified trimmed mean of the M-values normalization method and the unsupervised principal component analysis (PCA) was performed with DESeq2 Bioconductor package version 1.10.1 in R version 3.6.3. Each gene was fitted into a negative binomial generalized linear model, and the Wald test was applied to assess the differential expressions between two sample groups by DESeq2. Benjamini and Hochberg procedure was applied to adjust for multiple hypothesis testing, and differential expression gene candidates were selected with a false discovery rate less than 0.05. For visualization of coordinated gene expression in samples, a two-way hierarchical clustering with Pearson correlation distance matrix was performed with samples and differentially-expressed candidates using the Bioconductor g-plots package (version 3.0.3) in R. Gene ontology analysis and visualization conducted using REViGO online software.[37]

Beat rate analysis

Thirty-second video clips were taken of mock and infected hiPSC-CMs at 72 hours after viral infection. A beats-per-minute measurement was obtained by manually counting individual beats in a 30 s video and multiplying by 2 to extrapolate to 1 minute.

QUANTIFICATION AND STATISTICAL ANALYSIS

For statistical analyses, the Student's t test was used for comparison between two datasets. Excel or Prism software was used for statistical analysis. Data are presented as mean ± standard deviation as indicated in figure legends. A p value of < 0.05 is considered statistically significant and is denoted by *. Images used for statistical analysis were randomly chosen within a well of interest. Other statistical details can be found in figure legends. No data were excluded.

Supplemental Information

Human iPSC-Derived Cardiomyocytes
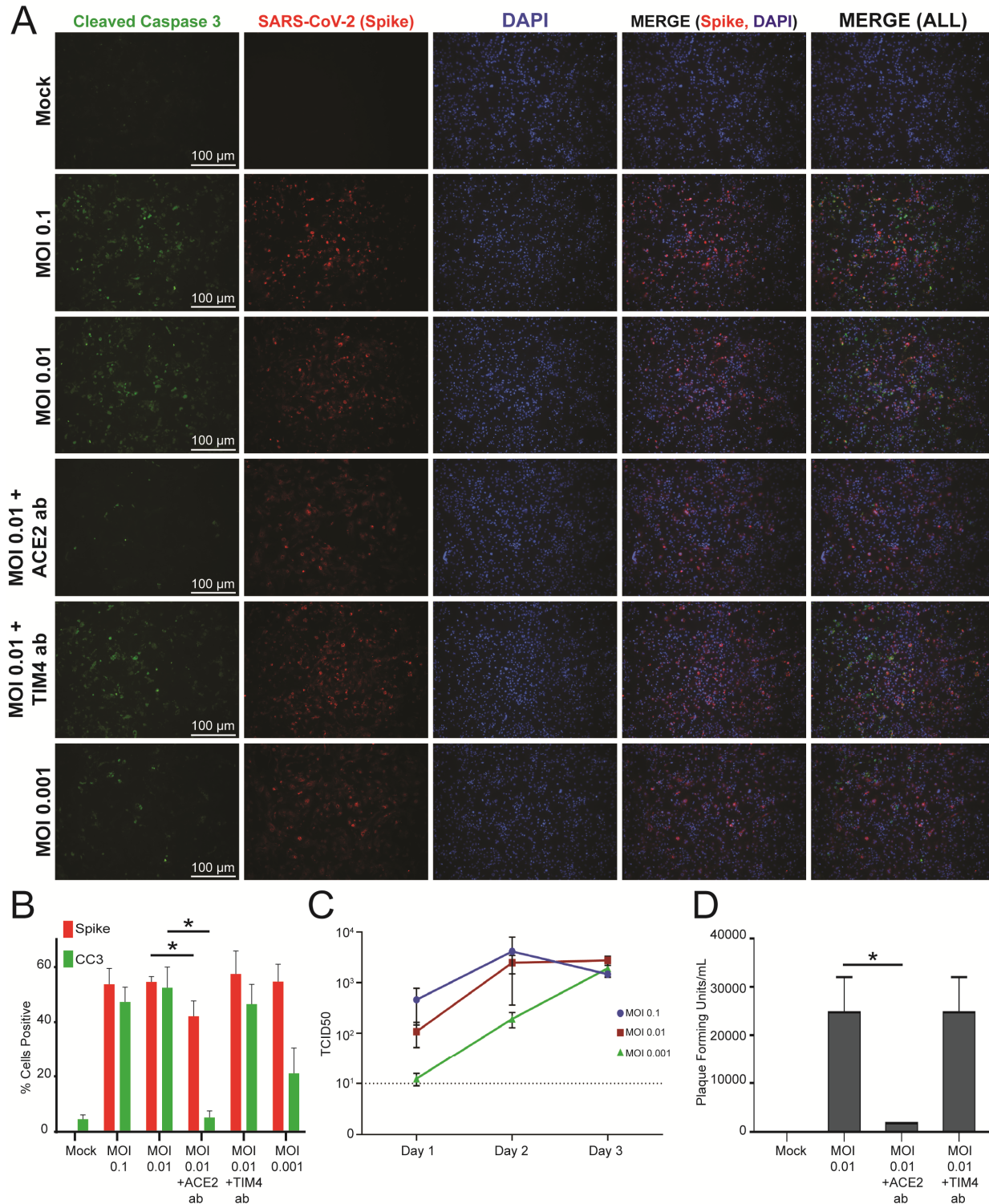
Are Susceptible to SARS-CoV-2 Infection

Arun Sharma, Gustavo Garcia Jr., Yizhou Wang, Jasmine T. Plummer, Kouki Morizono, Vaithilingaraja Arumugaswami, and Clive N. Svendsen

SUPPLEMENTAL INFORMATION

Human iPSC-Derived Cardiomyocytes are Susceptible to SARS-CoV-2 Infection

Arun Sharma, Gustavo Garcia Jr, Yizhou Wang, Jasmine T. Plummer, Kouki Morizono, Vaithilingaraja Arumugaswami, Clive N. Svendsen

Supplemental Figure 1: SARS-CoV-2 demonstrates dose-dependent infectivity on hiPSC-CMs, blunted by ACE2 antibody treatment. (Related to Figure 1). A) Immunofluorescence of infected hiPSC-CMs stained for apoptosis marker cleaved caspase-3 and SARS-CoV-2 spike protein. DAPI marks cell nuclei. Cells infected with SARS-CoV-2 for 3 days with MOI ranging from 0.001 to 0.1 exhibit viral protein expression and apoptosis. However, pre-treatment of infected hiPSC-CMs with ACE2 antibody significantly blunts spike protein and cleaved caspase-3 expression, suggesting the criticality of ACE2 in viral internalization. TIM4 antibody serves as a non-specific control. **B)** Quantification of immunofluorescence results. N=5 images quantified for each condition. DAPI was used to mark live cells for counting. * indicates $p < 0.05$. **C)** Viral infection kinetics timecourse using supernatant from infected hiPSC-CMs after 24-72 hours of SARS-CoV-2 infection confirms active viral production. $TCID_{50}$ (Median Tissue Culture Infectious Dose) determined per 25 microliters of supernatant. Dotted horizontal line shows detection limit. Uninfected samples did not have detectible viral load. **D)** Viral plaque assays conducted using supernatant from infected hiPSC-CMs after 72 hours of SARS-CoV-2 infection confirms active viral production, but blunted by ACE2 antibody treatment. * indicates $p < 0.05$